Dalton Transactions

A Hemilabile Manganese(I)-Phenol Complex and its Coordination Induced O–H Bond Weakening

Journal:	*Dalton Transactions*
Manuscript ID	DT-ART-03-2020-000973.R1
Article Type:	Paper
Date Submitted by the Author:	07-Apr-2020
Complete List of Authors:	Kadassery, Karthika; University at Buffalo, Chemistry Crawley, Matthew; University at Buffalo, Chemistry MacMillan, Samantha; Cornell University, Chemistry and Chemical Biology Lacy, David; University at Buffalo, Chemistry

Journal Name

ARTICLE

A Hemilabile Manganese(I)-Phenol Complex and its Coordination Induced O–H Bond Weakening

Received 00th March 2020,
Accepted 00th

DOI: 10.####/x0xx00000x

www.rsc.org/

Karthika J. Kadassery,[a] Matthew R. Crawley,[a] Samantha N. MacMillan,[b] David C. Lacy*[a]

Abstract: The known compound K[(**PO**)$_2$Mn(CO)$_2$] (**PO** = 2-((diphenylphosphino)methyl)-4,6-dimethylphenolate) (K[**1**]) was protonated to form the new Mn(I) complex (**HPO**)(**PO**)Mn(CO)$_2$ (^{H}**1**) and was determined to have a pK_a approximately equal to tetramethylguanidine (TMG). The reduction potential of K[**1**] was determined to be -0.58 V vs. Fc/Fc$^+$ in MeCN and allowed for an estimation of an experimental O–H bond dissociation free energy (BDFE$_{O–H}$) of 73 kcal/mol according to the Bordwell equation. This value is in good agreement with a corrected DFT computed BDFE$_{O–H}$ of 68.0 kcal/mol (70.3 kcal/mol for intramolecular H-bonded isomer). The coordination of the protonated O-atom in the solid-state ^{H}**1** was confirmed using FTIR spectroscopy and X-ray crystallography. The phenol moiety is hemilabile as evident from computation and experimental results. For instance, dissociation of the protonated O-atom in ^{H}**1** is endergonic by only a few kcal/mol (DFT). Furthermore, [**1**]$^-$ and other Mn(I) compounds coordinated to **PO** and/or **HPO** do not react with MeCN, but ^{H}**1** reacts with MeCN to form ^{H}**1+MeCN**. Experimental evidence for the solution-bound O-atoms of ^{H}**1** was obtained from ^{1}H NMR and UV-vis spectroscopy and comparing the electronic spectra of *bona fide* 16-e$^–$ Mn(I) complexes such as [{**PNP**}Mn(CO)$_2$] (**PNP** = $^-$N{CH$_2$CH$_2$(P^{i}Pr$_2$)}$_2$) and [(**Me$_3$SiOP**)(**PO**)Mn(CO)$_2$] (^{Me3Si}**1**). Compound ^{H}**1** is only meta-stable ($t_{1/2}$ 0.5 - 1 day) and decomposes into products consistent with homolytic O–H bond cleavage. For instance, treatment of ^{H}**1** with TEMPO resulted in formation of TEMPOH, free ligand, and [Mn^{II}{(**PO**)$_2$Mn(CO)$_2$}$_2$]. Together with the experimental and calculated weakened BDFE$_{O–H}$, these data provide strong evidence for the coordination and hemilability of protonated O-atom in ^{H}**1** and represents the first example of the phenolic Mn(I)–O linkage and a rare example of a "soft-homolysis" intermediate in the bond-weakening catalysis paradigm.

Introduction

The proton coupled electron transfer (PCET) chemistry induced by coordination of metal ions to phenolic O–H moieties is an important process in nature.[1,2] Additionally, others have recently taken advantage of "soft homolysis", or coordination induced X–H (X = O, N, etc.) bond weakening, for energy and chemical synthesis.[3-7] However, there are few reports on the thermodynamics of the O–H bond on phenolic ligands coordinated to a metal because phenols are weak ligands,[8] and covalent metal–Ph(O)H linkages are rare. Most metal–Ph(O)H are loosely bound ionic high-spin inorganic complexes, and the low-spin organometallic complexes contain 2nd and 3rd row transition-metal centers (for example, Mo,[9] Ru,[10] Rh,[11] and Ir[12]). Even high-spin compounds tend to deprotonate to give a phenolate-metal complex or, in the case of metallo-enzymes like transferrin,[1,2] undergo reductive PCET thus making the metastable phenol-bound metal complex difficult to isolate and characterize.[9,12c] Our ongoing efforts in studying O–H bond weakening in Mn(I) complexes and also development of phenolate-phosphine ligands led us to prepare a unique set of Mn(I)-phenol and phenolate complexes that are amenable to this study. As such, this report details a systematic thermodynamic evaluation of the first low-spin 1st-row transition metal-Ph(O)H motif. Herein, we describe the preparation of a Mn(I)–Ph(O)H complex, (**HPO**)(**PO**)Mn(CO)$_2$ (^{H}**1**), and discuss its solution and solid-state structure to demonstrate that the O-atom of the phenol is indeed coordinated to the Mn(I) center. This discussion then leads to an evaluation of the O–H bond dissociation free energy that is weakened from a free phenol as a result of the coordination.

Results and Discussion

Protonation of K[1] in non-coordinating solvents. In a previous report, we described the synthetic route to the anionic dicarbonyl Mn(I) complex supported with two **PO** ligands [(**PO**)$_2$Mn(CO)$_2$]$^-$ ([**1**]$^-$), where **PO** = 2-((diphenylphosphino)methyl)-4,6-dimethylphenolate; both the potassium and manganese(II) salt of [**1**]$^-$ were prepared (i.e. K[**1**] and Mn^{II}[**1**]$_2$).[13] Protonation of K[**1**] with one or more equivalents of lutidinium tetrafluoroborate ([Lt-H]BF$_4$) in DCM led to generation of a dark orange complex (**HPO**)(**PO**)Mn(CO)$_2$ (^{H}**1**), along with the formation of white ppt (KBF$_4$) (Scheme 1).[14] Monitoring the reaction with ^{31}P{^{1}H} NMR showed complete conversion from K[**1**] (^{31}P{^{1}H} NMR δ 55.2 ppm) to ^{H}**1**

[a] Department of Chemistry, University at Buffalo, State University of New York, Buffalo, New York 14260, United States E-mail: dclacy@buffalo.edu
[b] Department of Chemistry and Chemical Biology, Cornell University, Ithaca, New York 14853, United States
Electronic Supplementary Information (ESI) available: [details of any supplementary information available should be included here]. See DOI: 10.####/x0xx00000x

($^{31}P\{^1H\}$ NMR δ 54.3 ppm) (Figure S2). The ATR-FTIR spectrum of ^{H}**1** revealed that it is a dicarbonyl complex (ν_{CO} = 1924, 1844 cm^{-1}) with an OH stretch at 3480 cm^{-1} (Figure S3). The CO stretches are shifted to higher energy compared to that of K[**1**] (ν_{CO} = 1894, 1802 cm^{-1}). The ^1H NMR spectrum of ^{H}**1** contains a peak at δ 2.69 ppm that integrates to one proton, which is assigned to the OH group on the phenol (Figure S1a). This assignment was validated by the absence of this peak in the ^1H NMR spectrum of the deuterated analog (d_1-^{H}**1**) (Figure S1b). The ATR-FTIR of d_1-^{H}**1** showed the presence of a shifted OD stretch at 2580 cm^{-1} (ν(OH)/ν(OD) calc. = 1.37, exp. = 1.35) (Figure S4). Crystals suitable for diffraction were obtained using the deuterated analog d_1-^{H}**1** (Figure 1).[14] The XRD structure revealed a coordination environment similar to that of K[**1**]. While K[**1**] has a symmetrical structure with nearly equivalent Mn-O distances (2.075 and 2.068 Å), ^{H}**1** is comparatively asymmetric with nonequivalent Mn-O distances (2.210 and 2.014 Å) that is consistent with one of the O-atoms being protonated.

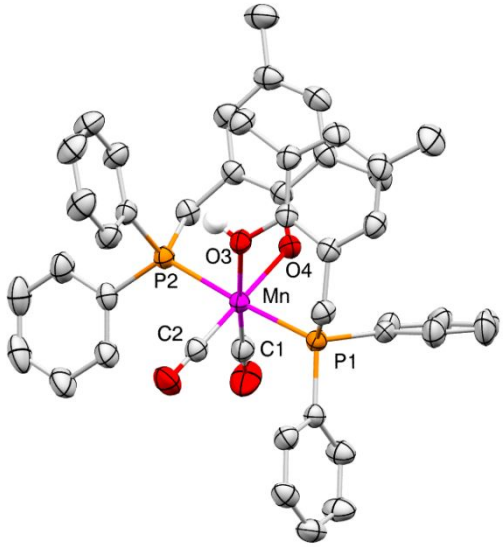

Fig. 1 Molecular structure of ^{H}**1** determined from XRD (ellipsoids at 50% probability). H-atoms attached to carbon not shown. Selected distances (Å): Mn–O4 = 2.014(1); Mn–O3 = 2.210(1); O3···O4 = 2.854(2); Mn–C1 = 1.762(2); Mn–C2 = 1.784(2); Mn–P1 = 2.292(1); Mn–P2 = 2.279(1).

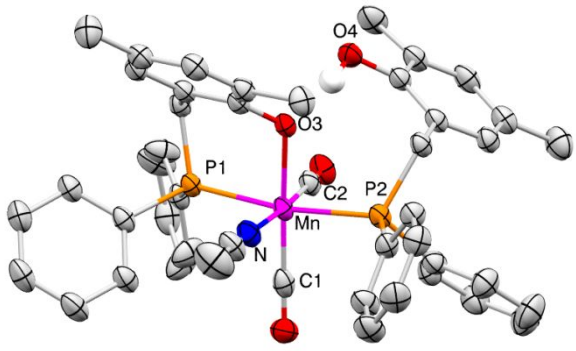

Fig. 2 Molecular structure of ^{H}**1+MeCN** determined from XRD (ellipsoids at 50% probability). H-atoms attached to carbon not shown. Selected distances (Å): Mn–O3 = 2.068(1); O3···O4 = 2.558(2); Mn–C1 = 1.778(2); Mn–C2 = 1.814(2); Mn–P1 = 2.3021(6); Mn–P2 = 2.3326(6); Mn–N = 1.997(2).

Scheme 1 Synthesis of ^{H}**1** and ^{H}**1+MeCN** from K[**1**]

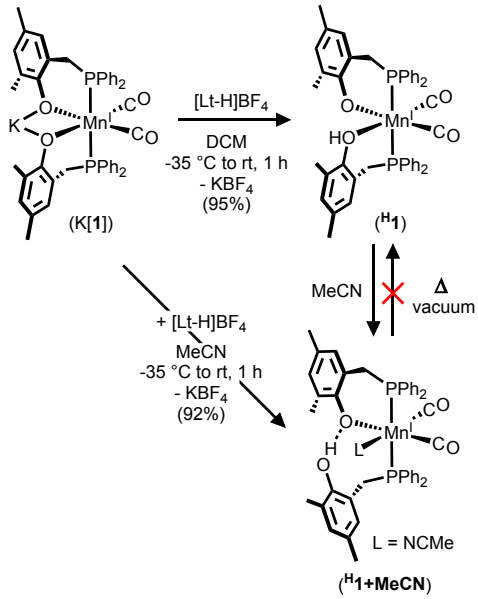

A DFT computed structure of ^{H}**1** (see Figure S5) is consistent with the XRD structure in which the phenol group coordinates to the vacant site *trans* to one of the CO ligands and *cis* to the phenolate and two phosphine ligands. Like the XRD structure, the DFT structure suggests different environments for the two phosphine ligands. Note that a different isomer was computed for ^{H}**1** in a previous report where the phenolic H-atom is engaged in an intramolecular H-bonding interaction (O_a–H···O_b).[13] This H-bonded isomer of ^{H}**1** is 2.7 kcal/mol lower in energy than the one without the H-bonding interaction (gas phase and in toluene).

It is possible that the solid-state and computed structures do not accurately describe the solution-state structure of ^{H}**1**. However, the OH ^1H-NMR chemical shift and ν_{OH} from FTIR are near those for the tetrameric Mn complex $[Mn(CO)_3(\mu_3\text{-}OH)]_4$ with bridging Mn-OH moieties.[15] The similarities indicate that the OH group is strongly interacting with a Mn(I) center, but the single $^{31}P\{^1H\}$ peak indicates a weak H-bonding interaction (O_a–H···O_b) or possible fluxional position of the proton (Figure S2a) in the solution state; NMR and UV-vis spectra of ^{H}**1** at low temperature were unchanged from room temperature.

An alternative solution-state structure is one where the phenol arm has dissociated away from the Mn(I) center resulting in a *bona fide* 16-e$^-$ 5-coordinate complex. This isomer of ^{H}**1** (^{H}**1'**) was computed as a local minimum using DFT, but it is 0.6 kcal/mol higher in energy than the one computed for ^{H}**1** and 3.3 kcal/mol higher than the intramolecular H-bonded isomer of ^{H}**1** (Scheme 4). Since VT NMR and UV-vis of ^{H}**1** did not indicate changes, we suspect that the H-bonded isomer of ^{H}**1** is predominant in the solution-state. Furthermore, as we will discuss, the electronic spectrum of ^{H}**1** appears to indicate that the O–H moiety is coordinated to Mn to effectively mask a 16-e$^-$ complex, rather than the dissociated 16-e$^-$ complex ^{H}**1'**.

Protonation of K[1] in coordinating solvents. Repeating the same protonation reaction of K[**1**] in acetonitrile led to dissociation of the protonated phenol group and association of a solvent molecule to give the neutral yellow compound (**HPO**)(**PO**)Mn(CO)$_2$(MeCN), (^{H}**1+MeCN**). This compound is isostructural with our previously reported complex (**HPO**)(**PO**)Mn(CO)$_3$, (^{H}**1+CO**).[13] The OH stretch in the ATR-FTIR spectrum (Figure S7) of ^{H}**1+MeCN** is broad and shifted to lower energy, 2350 cm^{-1}, suggesting a strong H-bond interaction with the

bound phenolate oxygen. $^{31}P\{^{1}H\}$ NMR spectrum of **^{H}1+MeCN** showed two broad peaks at δ 78.5 and 64.9 ppm corresponding to the bidentate **PO** ligand and the monodentate **HPO** ligand, respectively (Figure S6). These spectroscopic data closely match those associated with **^{H}1+CO**, which showed a similar broad OH peak at around 2500 cm^{-1} in the ATR-FTIR spectrum. The ^{1}H-NMR spectrum of **^{H}1+MeCN** was uninformative due to broadening from paramagnetic byproducts.[14] Crystals suitable for XRD were obtained (Figure 2). While addition of MeCN to solid **^{H}1** led to the formation of **^{H}1+MeCN**, the reverse reaction of removing a solvent molecule *in vacuo* from solid **^{H}1+MeCN** to form **^{H}1** did not occur (up to 75 °C, < 1 mTorr). Complexes **^{H}1+CO** and [**1**]$^{-}$ do not react with MeCN, thus providing some evidence that the ROH in **^{H}1** group is hemilabile to allow for the facile coordination of MeCN.

Hemilability of the phenol ligand in ^{H}1. Considering the weak binding of phenolic groups to metals, compound **^{H}1** can be thought of as a masked 16-e^{-} Mn(I) complex. The UV-vis spectrum of [**1**]$^{-}$ and other 18-e^{-} complexes prepared with **HPO** all contain a single large feature λ_{max} ≈ 400-500 nm, giving these complexes a yellow to orange color. However, **^{H}1** contains a new, but very weak, shoulder at 570 nm that is not present in any of the other complexes we observed so far and indicates a weakened ligand field (Figure 3).[16] We hypothesized that replacing the proton in **^{H}1** with other bulky electrophiles should allow us to generate unmasked 16-e^{-} complexes. Thus, we treated K[**1**] with Me_3SiOTf to yield a new deep-red compound *in situ*, assigned as (**Me_3SiOP**)(**PO**)$Mn(CO)_2$ (**^{Me3Si}1**)

Scheme 2 Synthesis of **^{Me3Si}1** from K[**1**]

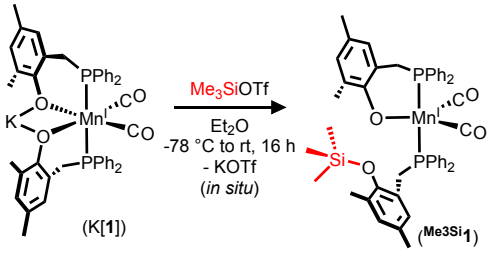

(Scheme 2). The $^{31}P\{^{1}H\}$ NMR spectrum showed two peaks at δ 51.7 and 51.9 ppm (Figure S8), and the ATR-FTIR spectrum revealed a dicarbonyl moiety (1925, 1851 cm^{-1}) (Figure S9), consistent with our assignment. Interestingly, the UV-vis spectrum of **^{Me3Si}1** contains two peaks at 400 and 550 nm, a feature that matches closely with Boncella's 16-e^{-} Mn(I) complex (**PNP**)$Mn(CO)_2$ (**PNP** = $^{-}$N{$CH_2CH_2(P^iPr_2)$}$_2$),[17] suggesting the true, unmasked 16-e^{-} nature of **^{Me3Si}1** (Figure 3). These changes in electronic structure are also consistent with those observed by others studying hemilabile Mn(I) and Ru(II) complexes.[16,18,19]

Collectively, the chemistry of **^{H}1** is consistent with a weakly coordinated, hemilabile Mn(I)-phenol complex. All spectroscopic (XRD, UV-vis, NMR, FTIR) point towards the phenol O-atom as coordinated in the solid and solution state, and DFT supports an uphill dissociation (≈ 1-3 kcal/mol) to form a dissociated species as a local minimum. Furthermore, the coordination of MeCN to **^{H}1**, but not **^{H}1+CO** or [**1**]$^{-}$, indicates that the phenol ligand undergoes facile ligand substitution.

Metastability of ^{H}1. Both **^{H}1** and **^{H}1+MeCN** are unstable and slowly convert into **^{H}1+CO** and other products regardless of solvent (DCM, MeCN, THF, toluene) with a half-life of about 0.5 - 1 day.[14] A similar degradation pattern was observed for a monocarbonyl d^6 Mo hemilabile phenol complex that decomposed into a dicarbonyl by an

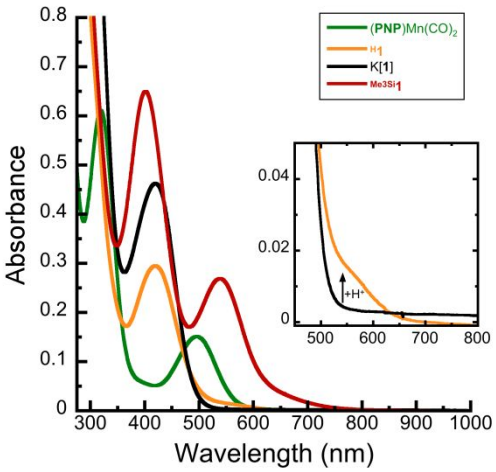

Fig. 3 UV-vis spectra of Mn(I) dicarbonyl compounds in benzene: λ_{max} K[**1**] = 420 nm (ε = 2700 $M^{-1}cm^{-1}$); **^{H}1** = 420 nm (shoulder = 570 nm); **^{Me3Si}1** = 402 nm, 540 nm; (**PNP**)$Mn(CO)_2$ = 319 nm, 496 nm. Inset shows the shoulder at 570 nm. **PNP** = $^{-}$N{$CH_2CH_2(P^iPr_2)$}$_2$.[17]

unknown path.[9] The conversion to **^{H}1+CO** appears to be linked to trace oxygen, but was initially puzzling since it is not a balanced reaction and since PCET and electron transfer between **^{H}1** and O_2 are both endergonic (*vide infra*). Free ligand is observed ($^{31}P\{^{1}H\}$ NMR δ -17.4 ppm), but there is no precipitate. We rationalized that the coordination of the phenolic O–H group to Mn(I), which is unprecedented, results in a weakened O–H bond and is responsible for the homolytic instability of **^{H}1**.

Scheme 3 H-atom transfer from **^{H}1** to TEMPO

5 [(**HPO**)(**PO**)$Mn(CO)_2$] (**^{H}1**) —(+ TEMPO; -TEMPOH; -2 **HPO**)→ 2 [(**HPO**)(**PO**)$Mn(CO)_3$] + Mn^{II}[**1**]$_2$ (**^{H}1+CO**)

We tested this hypothesis by addition of weak H-atom abstractors to **^{H}1**. For instance, **^{H}1** in DCM or toluene was treated with TEMPO and the products were analyzed using ^{1}H NMR, $^{31}P\{^{1}H\}$ NMR, ATR-FTIR, and headspace GC analysis (Figure S10). The ^{1}H NMR analysis showed the presence of TEMPOH, **^{H}1+CO**, and **HPO** in 1:2:2 ratio. Additionally, the ATR- FTIR spectrum revealed the presence of a previously reported compound Mn^{II}[**1**]$_2$, which is a paramagnetic trinuclear complex where a tetrahedral Mn^{II} ion links two [**1**]$^{-}$ molecular anions through the phenolate O-atoms.[13] No gaseous products were detected using headspace GC analysis. A balanced reaction for this H-atom transfer reaction from **^{H}1** to TEMPO is shown in scheme 3.

Interestingly, the reaction with **^{H}1** and TEMPO did not afford a complete O–H bond homolysis reaction. As we will show later, the experimental $BDFE_{O-H}$ of **^{H}1** is 2 kcal/mol higher than TEMPO ($BDFE_{O-H}$ = 66 kcal/mol), so unless the resulting Mn(II) species is unstable, the equilibrium established between **^{H}1** and TEMPO will lie towards the left; as will be described later, the Mn(II) species is indeed unstable and therefore consistent with the observed reactivity. However, **^{H}1** rapidly reacts with O_2 to form **^{H}1+CO** and other products. Although instability of organometallics with O_2 is not unusual, **^{H}1** is significantly more reactive toward O_2 than other Mn(I) **PO** or **HPO** complexes. Since the OH bond in O_2H (45 kcal/mol)[20] is even weaker than TEMPOH, the homolysis mechanism is probably not a straightforward simple H-atom transfer with O_2 and instead must involve additional processes, such as coordination of the H–atom acceptor or coupling to rapid and favorable secondary

decomposition reactions. Nevertheless, the general instability of ^{H}**1** is consistent with other unstable d^6 M-Ph(O)H complexes,[9,12c] and the reactivity is indicative of a weakened O–H bond, induced by the coordination of the phenol group to the metal and our efforts in determining the extent of this bond weakening is described next.

Estimating the BDFE$_{O-H}$ in ^{H}1. Coordination induced O–H bond weakening is well documented and we endeavored to experimentally determine the BDFE$_{O-H}$ in ^{H}**1** using Bordwell's equation (Scheme 4).[3,6,20,21] Ideally, a pK_a measurement should be carried out in polar solvents like MeCN, DMSO, DMF, water or methanol for which the C_G values in the Bordwell equation are known.[20] However, none of these polar coordinating solvents could be used for our pK_a determination. While MeCN generated ^{H}**1+MeCN**, DMSO, DMA, and DMF led to immediate decomposition to free ligand and other unidentified species, and methanol and water showed poor solubility of ^{H}**1**. The meta-stable complex ^{H}**1** is best handled in DCM or chloroform and thus we carried out the pK_a measurements in DCM using freshly prepared compounds. The pK_a of bases in MeCN have been found to be similar to those in DCM, which are taken as identical to those in THF and are linearly correlated (Table 1).[22,23,24]

Table 1. Relevant pK_a values in MeCN and DCM.¶

Base	pK_a MeCN[24,25,26]	pK_a THF or DCM[24]
DBU	24.3	20
TMG	23.3	17.8
Et_3N	18.5	13.7
DMAP	18.2	14.1
pyridine	12.5	8.3
aniline	10.6	8
DMF	6.1	1

¶ A plot of pK_a in MeCN vs. pK_a in DCM (or THF) gives a straight line with slope = 0.96 and y-intercept = 3.7 (R^2 = 0.98).

Thus, we treated ^{H}**1** with various bases in DCM and found that Et_3N (p$K_{a(MeCN)}$ = 18.5) showed no reaction, but one equivalent of DBU (p$K_{a(MeCN)}$ = 24.3) is sufficient to completely convert ^{H}**1** into a species consistent with [DBU-H][**1**] (Figure S11b). $^{31}P\{^{1}H\}$ NMR of the reaction mixture showed a new peak at δ 58.5 ppm (Figure S11a) shifted from that of both ^{H}**1** (δ 54.3 ppm) and K[**1**] (δ 55.2 ppm). The downfield shift of about 3 ppm observed for [DBU-H][**1**] with respect to K[**1**] suggests changes in the primary coordination environment, possibly arising from the replacement of the coordinating metal cation (K^+) with a non-coordinating organic cation ([DBU-H]$^+$). A similar downfield shift was observed for a reaction between K[**1**] and [PPN]Cl generating [PPN][**1**] (Figure S12).

$$^{H}\mathbf{1} + \text{TMG} \rightleftharpoons [\text{TMG-H}][\mathbf{1}] \qquad K_{eq} \sim 1$$

Reaction of ^{H}**1** with Et_3N and DBU narrowed the p$K_{a(MeCN)}$ range to be within 18.2 to 24.3. Hence, deprotonation of ^{H}**1** with equimolar TMG (p$K_{a(MeCN)}$ = 23.3) was performed and monitoring the reaction with $^{31}P\{^{1}H\}$ NMR showed two peaks corresponding to ^{H}**1** ($^{31}P\{^{1}H\}$ NMR δ 54.7 ppm) and [TMG-H][**1**] ($^{31}P\{^{1}H\}$ NMR δ 60.9 ppm) (Figure S13) in roughly equimolar amounts. ATR-FTIR of the reaction mixture showed carbonyl peaks corresponding to ^{H}**1** and [TMG-H][**1**] along with peaks corresponding to ^{H}**1+CO** in the baseline from decomposition (Figure S14). The reverse reaction by treating [PPN][**1**] with [TMG-H]BF_4 in $CDCl_3$ also showed production of ^{H}**1**, but with more decomposition to ^{H}**1+CO**. The meta-stability of ^{H}**1** (even under < 1 ppm O_2) made a precise equilibrium difficult to establish. Therefore, determining K_{eq} was not explicitly possible under the conditions studied here, but it is very close to 1 for the reaction with TMG and ^{H}**1**. Hence, the pK_a of ^{H}**1** is approximated to be very close to [TMG-H]$^+$ (Table 1).[24,26]

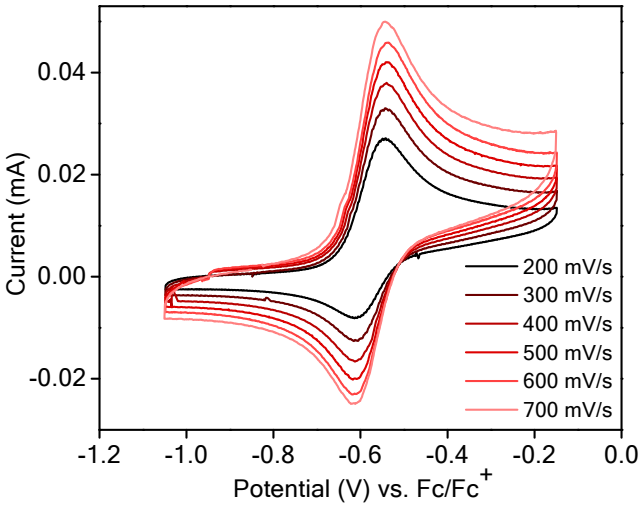

Fig. 4 Cyclic voltammogram of 0.001 M K[**1**] in MeCN at various scan rates. Experimental conditions: 0.1 M [Bu_4N][PF_6], glassy carbon working electrode, Ag/$AgNO_3$ reference electrode with a CoralPor™ separator, and platinum auxiliary electrode. $E_{1/2}$ = -0.58 V vs. Fc/Fc$^+$. Scan direction anodic.

Scheme 4 PCET thermochemistry of complex ^{H}**1**

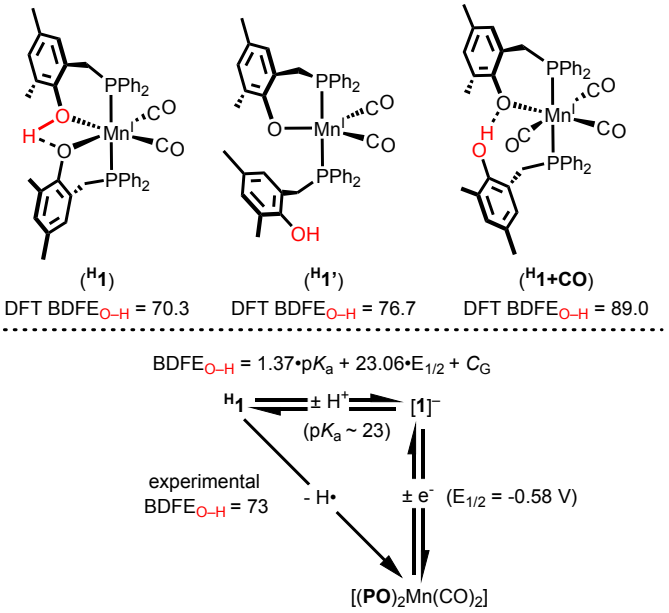

The reduction potential of [**1**]$^-$ was determined with cyclic voltammetry and was found to be -0.58 V vs. $FeCp_2$ in MeCN (Figure 4).[27] While there are known examples of meta-stable low-spin Mn(II) dicarbonyl compounds,[28,29] our limited attempts at isolating the product of [**1**]$^-$ oxidation (e.g., using $FeCp_2^+$ or NO^+) were unsuccessful despite the reversibility at moderately high scan rates; product of oxidation was mixtures of compounds including ^{H}**1+CO** (identified with FTIR) and unidentified paramagnets with EPR signals consistent with high-spin Mn(II) compounds (Figure S16).[13,29] Using the Bordwell equation, it is possible to estimate the MeCN BDFE$_{O-H}$ of ^{H}**1** (pK_a = 23 and $E_{1/2}$ = -0.58 V) to be 73 kcal/mol.

Since we could not precisely measure the acid/base equilibrium constant for [**1**]$^-$/^{H}**1** and used DCM instead of MeCN, we used DFT to support the viability of the estimated MeCN $BDFE_{O–H}$ for ^{H}**1**. For this, we computed the $BDFE_{X–H}$ (X = H, C, N, O) of several compounds for which the $BDFE_{X–H}$ is known and plotted the computed values vs. known experimental values (Figure 5).[20] This approach gives a straight line with which we can estimate a "corrected $BDFE_{O–H}$" for the complexes ^{H}**1**, ^{H}**1'**, and ^{H}**1+CO** (Scheme 4).[30] The uncorrected computed values were found to be 51.4 kcal/mol for ^{H}**1**, 54.3 kcal/mol for the H-bonded isomer of ^{H}**1**,[13] 62.1 kcal/mol for ^{H}**1'**, and 77.1 kcal/mol for ^{H}**1+ CO**, which when corrected are 68.0, 70.3, 76.7, and 89.0 kcal/mol for ^{H}**1**, H-bonded isomer of ^{H}**1**, ^{H}**1'**, and ^{H}**1+CO**, respectively (Scheme 4).

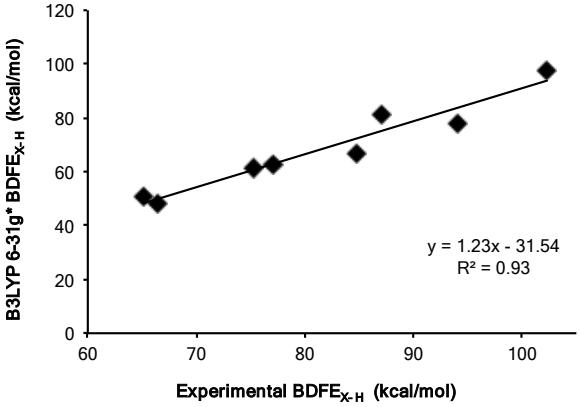

Fig. 5 Computed values of X–H (X = H, C, N, O) bond dissociation energies ($BDFE_{X–H}$) in kcal/mol plotted against known experimental values. The points used for this plot are taken from entries 1-8 in Table 2.

Table 2. Computed and Experimental $BDFE_{X–H}$ in MeCN.[a]

			$BDFE_{X–H}$ (kcal/mol)	
entry	**Compound**	**DFT**[b]	**Experimental**[c]	**corrected**
1	TEMPO–H	47.9	66.5	65.1
2	dtbuHA	51.4	65.2	68.0
3	TOC	61.7	75.2	76.4
4	2,4,6-ttbp	64.1	77.1	78.3
5	NHPI	65.5	84.8	79.5
6	aniline	79.6	94.1	91.0
7	toluene	81.7	87	92.7
8	H_2	92.08	102.3	101.2
-	^{H}**1+CO**	77.1	-	89.0
-	^{H}**1'**	62.1	-	76.7
-	^{H}**1** (w/ H-bond)	54.3	73	70.3
	^{H}**1** (no H-bond)	51.4	-	68.0

dtbuHA = *N,N*-di-*tert*-butylhydroxylamine; TOC = Trolox C; 2,4,6-ttbp = 2,4,6-tritertbutylphenol; NHPI = *N*-hydroxyphthalimide; [a] BDFE values are in kcal/mol, standard conditions. [b] B3LYP 6-31G* with SMD solvation model for MeCN. [c] experimental $BDFE_{O–H}$ from ref 20.

CONCLUSIONS

We have characterized the first example of a low-spin d^6 first-row transition metal complex containing a M–O linkage where the O-atom is from a phenol (M–Ph(O)H), namely in [(**HPO**)(**PO**)$Mn(CO)_2$] (^{H}**1**). Complexes like ^{H}**1** are rare because coordination of a phenolic O-atom destabilizes the O–H bond toward homolysis. This hypothesis was tested through a thermochemical analysis of the O–H bond strength in ^{H}**1** and observing its general chemical and physical properties. For instance, crystals of ^{H}**1** suitable for diffraction were only attainable for the deuterated species. The structure reveals that ^{H}**1** contains the first Mn(I)–O linkage where the O-atom is phenolic. The phenolic ligand is hemilabile, which was determined through DFT and its reactivity with MeCN ([**1**]$^-$ and ^{H}**1+CO** do not react with MeCN). Compound ^{H}**1** exhibited the hallmarks of homolytic instability, spontaneously decomposing into a mixture of species containing both ^{H}**1+CO** and Mn^{II}[**1**]$_2$, the latter of which is believed to have formed through decomposition initiated by a PCET reaction with ^{H}**1**. Some of the known d^6 2nd and 3rd row-transition M-Ph(O)H complexes exhibit similar thermal instability, and our work provides the first thermochemical analysis to provide one possible explanation. The decomposition of ^{H}**1** is accelerated by addition of TEMPO or small amounts of air, the former of which converts into TEMPOH. Of the isomers computed for ^{H}**1**, the lowest energy isomer contains an intramolecular H-bond. This isomer has a corrected calculated $BDFE_{O–H}$ of 70.3 kcal/mol and supports the estimated experimental value of 73 kcal/mol, which was obtained using Bordwell's equation in MeCN. We pursued the DFT analysis because we were unable to make precise pK_a measurements in DCM or in MeCN. The computed value for the 16-e$^-$ isomer ^{H}**1'** (corrected DFT value = 76.7 kcal/mol), which essentially has a free tri-substituted phenol, is close to that of 2,4,6-tritertbutylphenol (experimental value = 77.1 kcal/mol). Therefore, it is apparent how the coordination event lowers the $BDFE_{O–H}$. The higher value for ^{H}**1+CO** (computed 89.0 kcal/mol) is consistent with energy gained from the intramolecular O–H···O hydrogen bonding interaction. These data support the key hypothesis in soft-homolysis of coordination induced X–H bond weakening, a paradigm that has emerging utility in energy science and chemical synthesis.

EXPERIMENTAL SECTION

General Methods. All reagents were procured from commercial sources and were used without further purification unless otherwise noted. Solvents were purified and collected from a PPT solvent system and stored over 3 Å molecular sieves. Molecular sieves and basic alumina were activated at 200 °C under vacuum (<100 mTorr) for 48 hours before use. Unless noted, all the samples were prepared under nitrogen in a VAC Genesis glove box or under argon using standard Schlenk line techniques. Deuterated solvents were degassed by freeze-pump-thaw method and stored in the glove box in Strauss flasks. NMR experiments were performed on Varian Mercury-300 MHz, Inova-400 MHz, and Inova-500 MHz spectrometers. Transmission and ATR-FTIR spectra were collected inside of a VAC Atmospheres Omni glovebox using a Bruker Alpha IR spectrometer with ALPHA-P Platinum ATR module (diamond crystal). Cyclic voltammetry was obtained using a SP-200 Bio-Logic potentiostat. Headspace analysis was obtained using a PerkinElmer Clarus 580 GC (thermal conductivity detector, Ar carrier gas). EPR spectra were collected on a EMX Bruker X-band spectrometer on frozen solutions at 77 K. UV−vis spectra were collected using an 8154 Agilent Spectrophotometer. High resolution mass spectroscopy was performed in MeCN using an FT ICR Bruker 12 T mass spectrometer. Deuterated lutidinium tetrafluoroborate ([Lt-D]BF_4) was prepared by stirring [Lt-H]BF_4 in d_4-methanol for 12 h and removing the volatiles under vacuum. Compounds **HPO**, K[**1**], ^{H}**1+CO** and Mn^{II}[**1**]$_2$ were prepared according to previous literature.[13]

Computational Methods. All DFT calculations were performed using QChem 4.4,[31] and used the B3LYP functional, 6-31G* basis set, and SMD solvation model for MeCN and toluene. Geometry optimizations were performed using the crystal coordinates or manipulated/inputted in IQmol directly. Frequency calculations were performed on all structures to ensure no imaginary frequencies. Single point energy calculations were used to obtain the final electronic energy (enthalpy).

Synthesis of (HPO)(PO)Mn(CO)$_2$ (^{H}1). A solution of K[**1**]•(THF)$_3$ (90 mg, 0.09 mmol, 1.0 eq.) in DCM (2 mL) was cooled to -35 °C. A cold solution of [Lt-H]BF$_4$ (19 mg, 0.10 mmol, 1.1 eq.) in DCM (1 mL) was added dropwise. The solution immediately turned deep orange with the formation of white ppt. The reaction was allowed to stir for 1 h at rt. The solution was filtered using a fine frit and the ppt was washed with DCM. Removing the solvent from the red filtrate under vacuum yielded orange solid residue, which was washed with petroleum ether to remove the lutidine left behind. This orange solid was dried under vacuum to yield ^{H}**1** (64 mg, 95% yield). ^{1}H-NMR (d_2-DCM, 300 MHz, 298 K, ppm): δ 1.43 (s, 6H, CH_3), 2.16 (s, 6H, CH_3), 2.69 (s, 1H, OH), 3.71 (s, 4H, CH_2), 6.69 (s, 2H, CH), 6.72 (s, 2H, CH), 7.3-7.7 (20H, (C$_6H_5$)$_2$P). ^{31}P{^{1}H} NMR (d_2-DCM, 121 MHz, 298 K, ppm): δ 54.3 ppm. FTIR-ATR (cm^{-1}): 3480, 1923, 1844.

The deuterated compound d_1-^{H}**1** was synthesized following the above-mentioned procedure using [Lt-D]BF$_4$. Crystals suitable for XRD was obtained by layering a solution of d_1-^{H}**1** in DCM under petroleum ether.[14]

Synthesis of (HPO)(PO)Mn(CO)$_2$(MeCN) (^{H}1+MeCN). The acetonitrile bound complex (^{H}**1+MeCN**) was prepared using the following procedure. A solution of K[**1**]•(THF)$_3$ (90 mg, 0.09 mmol, 1.0 eq.) in MeCN (2 mL) was cooled to -35 °C. [Lt-H]BF$_4$ (19 mg, 0.10 mmol, 1.1 eq.) in MeCN was added while cold, during which the color changed from orange to yellow immediately along with precipitate formation. The reaction was allowed to stir at rt for 1 h. The solution was filtered using a glass fritted funnel and the precipitate collected. The precipitate was washed with MeCN. DCM was added to the material in the fritted funnel and filtered to collect a yellow filtrate, leaving behind a white residue. Removing volatiles from the filtrate under vacuum yielded ^{H}**1+MeCN** as yellow solid (65 mg, 92% yield). The DCM filtrate when layered under hexane and stored at -35 °C for one week to yield yellow crystals suitable for XRD. The compound ^{H}**1+MeCN** is either insoluble or sparingly soluble in common organic solvents like MeCN, THF, diethyl ether, benzene, toluene, acetone and methanol. Even though the compound tends to degrade in chlorinated solvents, its limited solubility in only DCM or chloroform required their use. ^{1}H NMR in chlorinated solvents led to broad peaks and inconclusive NMR data due to the presence of paramagnetic impurities arising from degradation.[14] ^{31}P{^{1}H} NMR (DCM, 121 MHz, 298 K, ppm): δ 78.5, 64.9 ppm. FTIR-ATR (cm^{-1}): 2330, 1941, 1862.

Elemental composition of ^{H}1 and ^{H}1+MeCN. Due to the instability of compound ^{H}**1** and ^{H}**1+MeCN**, CHN combustion analysis was not performed. Instead, HR-MS data were collected for a solution of ^{H}**1+MeCN** in MeCN prepared freshly from K[**1**], which showed the presence of ^{H}**1**+H$^+$ and ^{H}**1+MeCN**+H$^+$. Major peak; [M-MeCN+H]$^+$ [C$_{44}$H$_{42}$MnO$_4$P$_2$]$^+$ m/z$_{(found)}$ = 751.19625; m/z$_{(calculated)}$ = 751.19333. Minor peak; [M+H]$^+$ [C$_{46}$H$_{45}$MnNO$_4$P$_2$]$^+$ m/z$_{(found)}$=792.22293; m/z$_{(calculated)}$ = 792.21988.

pK_a estimation of ^{H}1. A solution of ^{H}**1** (10 mg, 0.01 mmol, 1.0 eq.) in DCM was treated with 1.0 eq. of base and the reaction was monitored using ^{31}P{^{1}H} NMR (SI figures).

***In situ* synthesis of (Me$_3$SiOP)(PO)Mn(CO)$_2$ (^{Me3Si}1)**. A solution of K[**1**] (15 mg, 0.02 mmol, 1.0 eq.) in ether (2 mL) was cooled to -78 °C. Me$_3$SiOTf (2.5 µL, 1.0 eq.) was added using a syringe. The color immediately turned deep red. The reaction was allowed to warm to rt overnight. The reaction mixture was filtered and the filtrate collected. ^{31}P{^{1}H} NMR (hexane, 121 MHz, 298 K, ppm): δ 51.7, 51.9 ppm. FTIR-ATR (cm^{-1}): 1925, 1851. This compound is thermally unstable and was not characterized further.

Conflicts of interest

The authors declare no competing financial interests.

Acknowledgements

Financial support was provided by the ACS Petroleum Research Fund ACS-PRF-57861-DN13 and NSF award #1847933. Karthika J. Kadassery gratefully acknowledges the Silbert fellowship for financial support. This work was completed using the resources of the University at Buffalo Chemistry Instrument Center (CIC).

Notes and references

1. S. Dhungana, C. H. Taboy, O. Zak, M. Larvie, A. L. Crumbliss, P. Aisen. Redox properties of human transferrin bound to its receptor. *Biochemistry* **2004**, *43*, 205-209. D. A. Lee, J. M. Goodfellow. The pH-induced release of iron from transferrin investigated with a continuum electrostatic model. *Biophys. J.* **1998**, *74*, 2747-2759.
2. D. A. Lee, J. M. Goodfellow. The pH-induced release of iron from transferrin investigated with a continuum electrostatic model. *Biophys. J.* **1998**, *74*, 2747-2759.
3. M. J. Bezdek, S. Guo, P. J. Chirik. Coordination-induced weakening of ammonia, water, and hydrazine X–H bonds in a molybdenum complex. *Science* **2016**, *354*, 730-733.
4. M.-C. Chang, K. A. Jesse, A. S. Filatov, J. S. Anderson. Reversible homolytic activation of water via metal-ligand cooperativity in a T-shaped Ni(II) complex. *Chem. Sci.* **2019**, *10*, 1360-1367.
5. K. J. Kadassery, K. Sethi, P. M. Fanara, D. C. Lacy. CO-Photolyis induced H-atom transfer from Mn(I)O–H bonds. *Inorg. Chem.* **2019**, *58*, 4679-4685.
6. S. Resa, A. Millan, N. Fuentes, L. Crovetto, M. L. Marcos, L. Lezama, D. Choquesillo-Lazarte, V. Blanco, A. G. Campana, D. J. Cardenas, J. M. Cuerva. O–H and (CO)N–H bond weakening by coordination to Fe(II). *Dalton Trans.* **2019**, *48*, 2179-2189.
7. E. C. Gentry, R. R. Knowles. Synthetic applications of proton-coupled electron transfer. *Acc. Chem. Res.* **2016**, *49*, 1546-1556.
8. V. Ryzhov, R. C. Dunbar. Interactions of phenol and indole with metal ions in the gas phase: Models for Tyr and Trp side-chain binding. *J. Am. Chem. Soc.* **1999**, *121*, 2259-2268.
9. Tamm, M.; Bannenberg, T.; Dressel, B.; Fröhlich, R.; Holst, C., Molybdenum Complexes with Linked Cycloheptatrienyl Phenolate Ligands. *Inorg. Chem.* **2002,** *41*, 47-59.
10. (a) Biancalana, L.; Ciancaleoni, G.; Zacchini, S.; Monti, A.;

Marchetti, F.; Pampaloni, G., Solvent-Dependent Hemilability of (2-Diphenylphosphino)Phenol in a Ru(II) para-Cymene System. *Organometallics* **2018,** *37*, 1381-1391. (b) Wong, C.-Y.; Man, W.-L.; Wang, C.; Kwong, H.-L.; Wong, W.-Y.; Lau, T.-C., Proton-Bridged Dinuclear (salen)Ru Carbene Complexes: Synthesis, Structure, and Reactivity of {[(salchda)RuC(OR)(CHCPh2)]2·H}+. *Organometallics* **2008,** *27*, 324-326. (c) Booysen, I. N.; Maikoo, S.; Akerman, M. P.; Xulu, B., Isolation of ruthenium compounds with bidentate benz(imidazole/othiazole) chelators. *Transit. Met. Chem.* **2015,** *40*, 397-404. (d) Aneetha, H.; R. K. Rao, C.; Mohan Rao, K.; S. Zacharias, P.; Feng, X.; C. W. Mak, T.; Srinivas, B.; Y. Chiang, M., Synthesis and molecular structure of di- and mono-nuclear Schiff-base phenolate complexes: facile formation of cyclometallated ruthenium complexes. *J. Chem. Soc., Dalton Trans.* **1997,** *10*, 1697-1704. (e) Schlindwein, S. H.; Hänisch, S.; Nieger, M.; Gudat, D., Ruthenium Catechol Phosphane Complexes as Metalloligands for the Controlled Assembly of Heterobimetallics. *Eur. J. Inorg. Chem.* **2017**, *32*, 3834-3842.

11. (a) Siefert, R.; Weyhermüller, T.; Chaudhuri, P., Isolation, structural and spectroscopic investigations of complexes with tridentate [O,P,O] and [O,O,O] donor ligands. *J. Chem. Soc., Dalton Trans.* **2000**, *24*, 4656-4663. (b) Stinziano-Eveland, R. A.; Nguyen, S. T.; Liable-Sands, L. M.; Rheingold, A. L., Synthesis and Characterization of Rhodium(III) Dichloro Complexes with Unsymmetrically Bound Salen-Type Ligands. *Inorg. Chem.* **2000,** *39*, 2452-2455. (c) Inoue, H.; Ito, J.-i.; Kikuchi, M.; Nishiyama, H., Asymmetric Ligand-Exchange Reaction of Biphenol Derivatives and Chiral Bis(oxazolinyl)phenyl–Rhodium Complex. *Chemistry – An Asian Journal* **2008**, *3*, 1284-1288.
12. (a) Wang, Y.; Huang, Z.; Leng, X.; Zhu, H.; Liu, G.; Huang, Z., Transfer Hydrogenation of Alkenes Using Ethanol Catalyzed by a NCP Pincer Iridium Complex: Scope and Mechanism. *J. Am. Chem. Soc.* **2018,** *140*, 4417-4429. (b) Kuwabara, T.; Tezuka, R.; Ishikawa, M.; Yamazaki, T.; Kodama, S.; Ishii, Y., Ring Slippage and Dissociation of Pentamethylcyclopentadienyl Ligand in an (η5-Cp*)Ir Complex with a κ3-O,C,O Tridentate Calix[4]arene Ligand under Mild Conditions. *Organometallics* **2018,** *37*, 1829-1832. (c) Ringenberg, M. R.; Rauchfuss, T. B., Protonation-Enhanced Lewis Acidity of Iridium Complexes Containing Noninnocent Amidophenolates. *Eur. J. Inorg. Chem.* **2012,** *2012* (3), 490-495.
13. Kadassery, K. J.; MacMillan, S. N.; Lacy, D. C., Resurgence of Organomanganese(I) Chemistry. Bidentate Manganese(I) Phosphine–Phenol(ate) Complexes. *Inorg. Chem.* **2019,** *58* (16), 10527-10535.
14. The compounds ^{H}**1** and ^{H}**1+MeCN** are unstable and the degradation of these complexes led to the formation of ^{H}**1+CO**, free ligand, and a paramagnetic compound Mn^{II}[**1**]$_2$; these degradations occurred even under rigorous exclusion of O_2 (< 1 ppm) but was accelerated by dry air, and ^{H}**1+MeCN** is only meta-stable in chlorinated solvents. Several attempts to grow crystals of ^{H}**1** failed due to instability and was only possible for the deuterated analogue of ^{H}**1**. ^{1}H NMR of these, especially of ^{H}**1+MeCN**, were often significantly broadened from paramagnetic impurities (probably Mn^{II}[**1**]$_2$).
15. Kadassery, K. J.; Dey, S. K.; Friedman, A. E.; Lacy, D. C., Exploring the Role of Carbonate in the Formation of an Organomanganese Tetramer. *Inorg. Chem.* **2017,** *56* (15), 8748-8751.
16. Hartl, F.; Rosa, P.; Ricard, L.; Le Floch, P.; Záliš, S., Electronic transitions and bonding properties in a series of five-coordinate "16-electron" complexes $[Mn(CO)_3(L_2)]^-$ (L_2=chelating redox-active π-donor ligand). *Coordin. Chem. Rev.* **2007,** *251*, 557-576.
17. Tondreau, A. M.; Boncella, J. M., 1,2-Addition of Formic or Oxalic Acid to –N{CH2CH2(PiPr2)}2-Supported Mn(I) Dicarbonyl Complexes and the Manganese-Mediated Decomposition of Formic Acid. *Organometallics* **2016,** *35* (12), 2049-2052.
18. J. C. Jeffrey, T. B. Rauchfuss. Metal complexes of hemilabile ligands. Reactivity and structure of dichlorobis(o-(diphenylphosphino)anisole)ruthenium(II). *Inorg. Chem*. **1979,** *18*, 2658-2666.
19. (a) Bader, A.; Lindner, E. Coordination chemistry and catalysis with hemilabile oxygen-phosphorus ligands. *Coord. Chem. Rev.* **1991**, *108*, 27-110. (b) Braunstein, P.; Naud, F. Hemilability of Hybrid Ligands and the Coordination Chemistry of Oxazoline-Based Systems. *Angew. Chem. Int. Ed.* **2001**, *40*, 680-699.
20. Warren, J. J.; Tronic, T. A.; Mayer, J. M., Thermochemistry of Proton-Coupled Electron Transfer Reagents and its Implications. *Chem. Rev.* **2010,** *110* (12), 6961-7001.
21. (a) Jonas, R. T.; Stack, T. D. P., C−H Bond Activation by a Ferric Methoxide Complex: A Model for the Rate-Determining Step in the Mechanism of Lipoxygenase, *J. Am. Chem. Soc.* **1997**, *119*, 8566−8567. (b) Cuerva, J. M.; Campana, A. G.; Justicia, J.; Rosales, A.; OllerLopez, J. L.; Robles, R.; Cardenas, D. J.; Bunuel, E.; Oltra, J. E., Water: The Ideal Hydrogen-Atom Source in Free-Radical Chemistry Mediated by Ti^{III} and Other Single-Electron-Transfer Metals?, *Angew. Chem., Int. Ed.* **2006**, *45*, 5522−5526. (c) Chciuk, T. V.; Flowers, R. A. II, Proton-Coupled Electron Transfer in the Reduction of Arenes by SmI_2-Water Complexes. *J. Am. Chem. Soc*. **2015**, *137*, 11526−11531.
22. Li, T.; Lough, A. J.; Morris, R. H. An acidity scale of tetrafluoroborate salts of phosphonium and iron hydride compounds in [D_2]dichloromethane. *Chem. Eur. J.* **2007**, *13*, 3796-3803.
23. Morris, R. H. Estimating the acidity of transition metal hydrides and dihydrogen complexes by adding ligand acidity constants. *J. Am. Chem. Soc.* **2014**, *136*, 1948-1959.
24. Morris, R. H. Bronsted-Lowry acid strength of metal hydrides and dihydrogen complexes. *Chem. Rev.* **2016**, *116*, 8588-8654.
25. Kaljurand, I.; Kütt, A.; Sooväli, L.; Rodima, T.; Mäemets, V.; Leito, I.; Koppel, I. A. Extension of the Self-Consistent

Spectrophotometric Basicity Scale in Acetonitrile to a Full Span of 28 pKa Units: Unification of Different Basicity Scales. *J. Org. Chem*. **2005**, *70*, 1019–1028.

26. (a) Kaupmees, K.; Trummal, A.; Leito, I., Basicities of Strong Bases in Water: A Computational Study. *Croat. Chem. Acta.* **2014**, *87* (4), 385-395. (b) Binkowska, I.; Jarczewski, A. Formation of carbanions derivatives of C-acids activated by sulfonyl groups in the presence of organic bases in acetonitrile and tetrahydrofuran. *J. Mol. Structure*. **2008,** *875*, 86-90. (c) Kolthoff, I. M.; Chantooni Jr., M. K.; Bhowmik, S. Dissociation constants of uncharged and monovalent cation acids in dimethyl sulfoxide. *J. Am. Chem. Soc.* **1968**, *90*, 23-28.
27. The CV of [**1**]$^{-}$ in DCM contained ill-defined, broad redox events.
28. For instance: R. H. Reimann, E. Singleton. A simple route to some carbonyl and metal phosphine salts using $NOPF_6$. *J. Organometallic Chem.* **1971**, *32*, C44-C46.
29. P. H. Rieger. Electron paramagnetic resonance studies of low-spin d^5 transition metal complexes. *Coord. Chem. Rev.* **1994**, *135/136*, 203-286.
30. (a) Matson, B. D.; Peters, J. C., Fe-Mediated HER vs N_2RR: Exploring Factors That Contribute to Selectivity in $P_3^EFe(N_2)$ (E = B, Si, C) Catalyst Model Systems. *ACS Catal.* **2018,** *8*, 1448-1455. (b) Chalkley, M. J.; Oyala, P. H.; Peters, J. C., Cp* Noninnocence Leads to a Remarkably Weak C–H Bond via Metallocene Protonation. *J. Am. Chem. Soc.* **2019,** *141*, 4721-4729.
31. Shao, Y. et. al. *Mol. Phys*. **2015** *113*, 184–215.

(^{H}**1**)

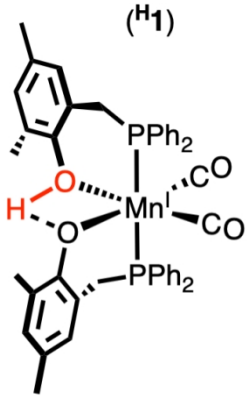

DFT $BDFE_{O–H}$ = 70.3
Experimental $BDFE_{O–H}$ = 73

(^{H}**1'**)

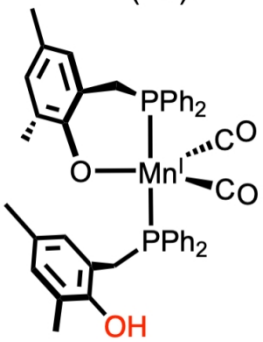

DFT $BDFE_{O–H}$ = 76.7

(^{H}**1+CO**)

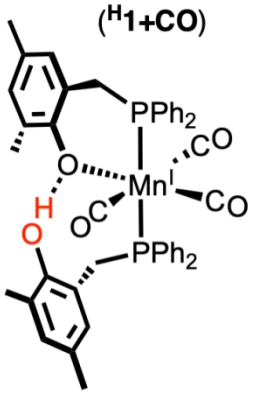

DFT $BDFE_{O–H}$ = 89.0